JBUON 2019; 24(1): 347-353
ISSN: 1107-0625, online ISSN: 2241-6293 • www.jbuon.com
E-mail: editorial_office@jbuon.com

ORIGINAL ARTICLE

Potential of utilization of albumin as a delivery module in cancer model

Zhe Jin[1], Jin-Sheng Li[2], Da-Nian Tang[3]

[1]State Key Laboratory of Biomembrane and Membrane Biotechnology, School of Medicine, Tsinghua University, Haidian District, Tsinghua East Street, Beijing 100084, People's Republic of China; [2]Emergency Department, Aviation General Hospital (361), Chaoyang District, Anwaibeiyuan No.3, Beijing100012, People's Republic of China; [3]Gastro-Intestinal Surgery Department, Beijing Hospital, Dongcheng District, Dongdandahua Road, Beijing 100730, People's Republic of China.

Summary

Purpose: *This study compared the potential of 2 nanoparticles, namely albumin and gold nanoparticles, for the specific delivery of ^{99m}TC- resveratrol in colon cancer. The aim of adding radioactive tag (^{99m}TC) to resveratrol was to utilize it for imaging purposes.*

Methods: *We compared the potential of albumin loaded ^{99m}TC- resveratrol with gold nanoparticles loaded ^{99m}Tc-resveratrol for tumor specific delivery. Twenty male Wistar rats were used for the formation of colon cancer model. Both delivery molecules were tested for tumor specific delivery.*

Results: *The results showed efficient delivery of ^{99m}TC-resveratrol with albumin in comparison to gold nanoparticles, as confirmed by single-photon emission computed tomography (SPECT).*

Conclusions: *Albumin is a superior molecule for the efficient delivery of ^{99m}TC- resveratrol at tumor sites in comparison to gold nanoparticles.*

Key words: *albumin, colon cancer, gold nanoparticles, siRNA, ^{99m}Tc*

Introduction

Molecular imaging using radionuclides involves an imaging device and an imaging agent, known as radiopharmaceutical. This radiopharmaceutical provides detailed picture at both the molecular and cellular levels [1]. The chemical processes involved in metabolism, oxygen use or blood flows are easily visible with the help of molecular imaging [2]. It is well known that the biochemical activities of cells begin to change during carcinogenesis. For instance, cancer cells multiply at a much faster rate and are more active in comparison to normal cells. So, radiopharmaceuticals are designed to target such cancer specific changes, in order to localize the cancerous lesions in the physiological system [3]. The dietary anticancer agent resveratrol has shown its anticancer properties without any side effects in earlier studies [4,5]. So, we have used resveratrol as novel conjugate for tagging of ^{99m}Tc, as a stable conjugate is essential for the *in vivo* stability of the radiopharmaceutical [6]. This new radiopharmaceutical could serve the purpose of imaging of premalignant lesions in the colon cancer model. Furthermore, we have exploited two nanoparticles, namely. albumin and gold nanoparticles for the purpose of targeting specific delivery of ^{99m}Tc-resveratrol and compared their efficacies as well.

Albumin is emerging as a versatile protein carrier for drug targeting and for improving the pharmacokinetic profiles of peptide- or protein-

Correspondence to: Dr. Da-Nian Tang. Gastro-Intestinal Surgery Department, Beijing Hospital, Dongcheng District, Dongdandahua Road, Beijing 100730, People's Republic of China.
E-mail: tangdn@126.com
Received: 01/09/2018; Accepted: 28/09/2018

based drugs [7,8]. Albumin is the most abundant plasma protein (35–50 g/L human serum) with a molecular weight of 66.5 kDa. The biological application of nanoparticles is a rapidly developing area of nanotechnology that raises new possibilities in the diagnosis as well as in the treatment of cancer [9,10]. Like most of the plasma proteins, albumin is synthesized in the liver where it is produced at a rate of approximately 0.7 mg/h for every gram of liver (i.e. 10–15 g daily); Human serum albumin (HSA) with an average half-life of 19 days exhibits multiple functions and has excellent binding properties. On the other hand, gold nanoparticles are already well known for their drug delivery capabilities [11]. However, there are some reports for *in vivo* toxicity caused by gold nanoparticles [12,13]. Therefore, there is an urgent need of an endogenous nanoparticle with least toxicity for the delivery of drugs. In this scenario of least toxicity and high efficacy, serum albumin holds good potential. We have utilized serum albumin as a delivery molecule for ^{99m}TC- resveratrol in the present study. So, in the present study, we have focused on the efficacies of both nanoparticles in terms of sensitivity as well as specificity at tumor sites.

Methods

Chemicals

All chemicals, reagents etc. were procured from Sigma Aldrich Co (St.Louis, USA).

Animals

Twenty male Wistar rats weighing 140-160g were procured for the designed experiments. Another set of 20 rats weighing 140-160 g was procured from Central Animal House of Tsinghua University for radio-tagging experiment. All the animals were housed in polypropylene cages under hygienic conditions in the departmental animal house by strictly following the guidelines as outlined by the institutional ethical committee.

Experimental design

Animals were segregated equally and randomly into 2 treatment groups. Animals in group I served as normal controls. Animals in group II were injected with dimethyl hydrazine (DMH) subcutaneously at a dose of 30mg/kg body weight/week for a total duration of 20 weeks [14]. DMH is a carcinogen used for induction of colon cancers in rats. All the animals had free access to diet and water and the treatments continued for the total duration of the study. After 20 weeks, half of group II animals were treated with albumin-^{99m}Tc-resveratrol and half were treated with gold nanoparticles loaded ^{99m}Tc-resveratrol.

Formation of albumin tagged ^{99m}Tc-resveratrol complex

^{99m}Tc-resveratrol was prepared by adding 3.7 in megabequerel (MBq) (100μCi) of ^{99m}TcO4- to a vial containing 100 μg of trans-resveratrol (1mg/ml solution in 10% ethanol) and 50 μg of albumin. To the mixture, 100μg of SnCl2•2H2O (1 mg/ml solution in 0.1N HCl) was added and the pH was adjusted to 5-5.5 with 0.05 M NaHCO3. The reaction mixture was vortexed and kept at ambient temperature for a sufficient time to complete the reaction. Optimization of reaction time, chemical constituents such as SnCl2•2H2O, albumin, resveratrol, and ^{99m}TcO4- activity as well as the stability of the resultant complex with pH and time, was investigated in order to maximize the radiochemical yield.

Formation of gold nanoparticles loaded ^{99m}Tc-resveratrol

Gold nanoparticles (AuNPs) were synthesized using the method described in 2009 by Nune et al. [15], which involves reduction of NaAuCl4, the precursor with gum arabic (GA), which served both as a reducing and a stabilizing agent in the synthesis reaction. A range of calculated amount of resveratrol was added to the dispersion of gold nanoparticles obtained as described above, resulting in a final resveratrol concentration of 10-8 to 102 M in solution. The mixture was then allowed to react at room temperature for 24 hrs. To separate free unloaded resveratrol from loaded AuNPs, the mixture was centrifuged at 15,000 rpm for 60 min. The supernatant thus obtained was used for quantification of free resveratrol, using UV spectroscopy. The pellets were resuspended in double distilled water and centrifuged at 15,000 rpm for 60 min twice again to completely remove free resveratrol and other impurities and then carefully separated from the supernatant and redispersed in distilled water. Finally, the solution was freeze-dried to obtain the resveratrol loaded gold nanoparticles (Res-AuNPs) in the form of a fine powder that was highly soluble in water and fairly soluble in dimethylsulphoxide (DMSO). In order to imaging Res-AuNPs, they were radiolabeled with ^{99m}Tc using stannous chloride reduction method as described previously for the synthesis of albumin tagged-^{99m}Tc-resveratrol.

Biodistribution and radionuclide imaging

Biodistributions of both ^{99m}Tc-Res-AuNP and albumin-^{99m}Tc-reseveratol were carried out in DMH-treated, colon tumor-bearing rats following i. v. administration of both complexes. Percent specific uptake values for different organs at different time points from 0.25 to 4 hrs were evaluated for both the complexes. Radionuclide imaging was carried out for colon tumor-bearing rats using micro single photon emission computed tomography (SPECT).

Statistics

The statistical significance of the data was determined using one-way analysis of variance (ANOVA), followed a multiple *post-hoc* least significant difference test, and the results are presented as means ± SD. The statistical analysis was carried out by using SPSS 12 statistical

software package (SPSS Inc. Chicago. Il). Statistical significance was considered at a level of $p < 0.05$.

Results

The results obtained from various experiments conducted in this study are shown in Figures 1-6. The data from the treatment group have been compared with the normal control animals.

Morphometric/gross analysis of colon

The tumor incidence and tumor multiplicity observed in rat colon after 20 weeks of DMH treatment were found to be 85±5% and 2.87±0.64 per rat, respectively. The average volume of the tumors was found to be 2.04±0.04 cm^3. No tumors were observed in colon of control rats (Figure 1).

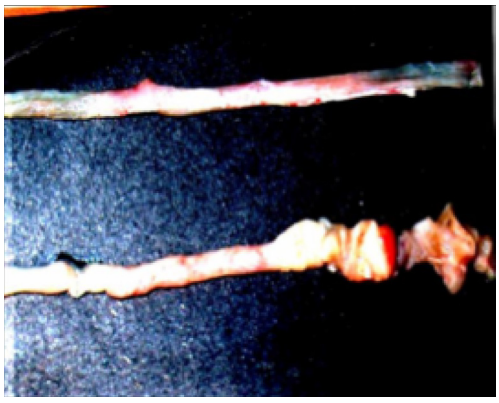

Figure 1. Excised colons from rats

Histopathological examination of colon tissue sections

The paraffin-embedded sections of colon were critically examined under light microscope following hematoxylin and eosin staining (H/E) (Figure 2). Transverse sections of the rat colon at 40x obtained from control and DMH treated rats are shown in Figure 2. Colon sections from control rats depicted normal histo-architecture with no signs of abnormality. Crypts with single layered nuclei of normal size and shape were observed. Histopathological analysis of DMH-treated colon sections showed well differentiated signs of neoplasia (new abnormal cell formation) with moderately differentiated adenocarcinoma which was characterized by multilayered pleomorphic nuclei and presence of glandular lumina.

Biodistribution and imaging of goldparticles loaded ^{99m}TC resveratrol

Following i.v. administration of ^{99m}Tc-Res-AuNPs through the penile vein in control rats (Figure 3a), the radiotracer was quickly taken up by the liver, spleen, urinary bladder and kidneys. An initial rise for 2 hrs followed by a fall thereafter in kidney and liver uptake and a constant increase in spleen uptake was observed over 4 hrs. Significantly low percent specific uptake values when compared to liver, kidney, spleen and bladder uptake values were observed in all the other organs including stomach and thyroid which decreased gradually from 0.25 to 4 hrs.

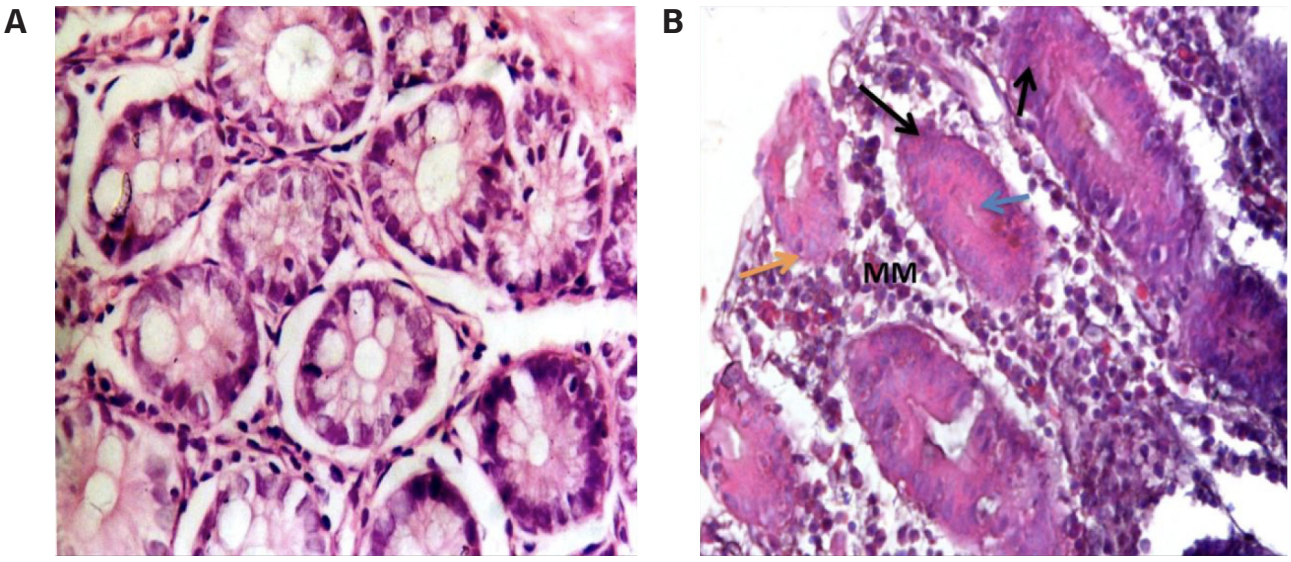

Figure 2. Histological changes induced in rat colon tissue after 16 weeks of DMH treatment. Light microscopic view of H/E stained transverse sections of rat colon (40x). **(A)** normal single layered glandular cells, uniform nucleus size indicating normal histo-architecture with no signs of apparent abnormality; **(B)**Histopathological analysis of DMH treated colon sections show well differentiated signs of neoplasia (new abnormal cell formation) with moderately differentiated adenocarcinoma which is characterized by multi-layered (black arrows) pleomorphic (variability in size) (orange arrow) nuclei and presence of glandular lumina (blue arrow). MM-muscularis mucosa.

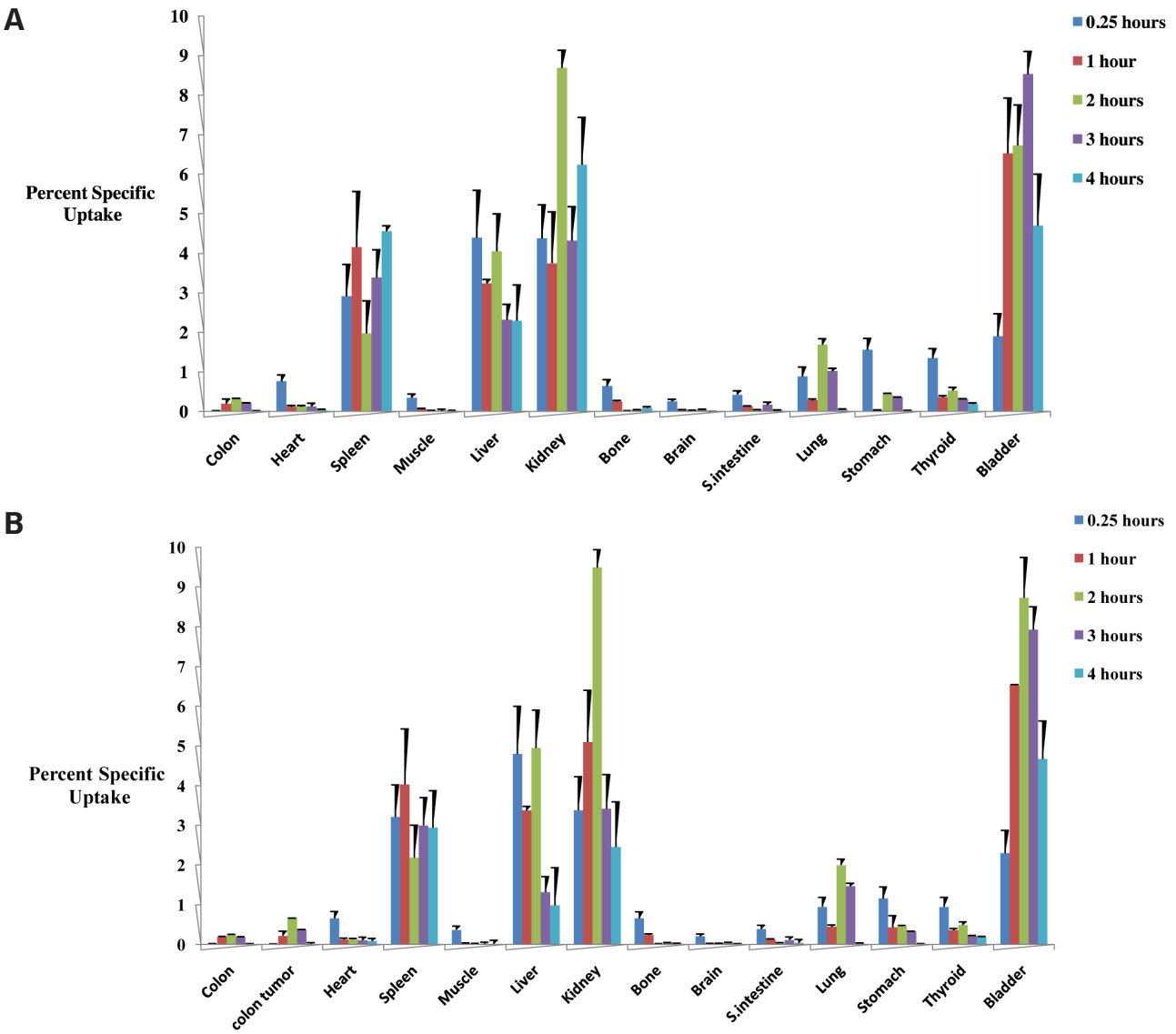

Figure 3. (A) Biodistribution of gold particles loaded ^{99m}TC resveratrol in controls. Using Gamma ray counter the radiotracer was quickly taken up by the liver, spleen, urinary bladder and kidneys and a constant increase in spleen uptake was observed over 4 hrs. **(B)** Biodistribution of gold particles loaded ^{99m}TC resveratrol in colon cancer rats. Using Gamma ray counter significantly higher percent values of age-speciafic uptake ($p \leq 0.01$) were obtained in colon tumors compared to normal colon tissue of the same group and control group after 2 and 3 hrs of administration of the radiopharmaceutical.

As shown in Figure 3b, significantly higher percent values of age-specific uptake ($p \leq 0.01$) were obtained in colon tumors compared to normal colon tissue of the same group and control group after 2 and 3 hrs of administration of the radiopharmaceutical. Furthermore, the biodistribution at all time points, in all the other organs was similar to that observed in control rats. In addition, SPECT images also confirmed similar results (Figure 4).

Biodistribution and imaging of albumin tagged ^{99m}TC resveratrol

Following i.v. administration of albumin tagged ^{99m}TC resveratrol (Figure 5) through the penile vein in rats, the radiotracer was quickly taken up by the liver, spleen, kidneys and soon appeared in urine (urinary bladder) after 15 min of i.v. injection. An initial fall in kidney, spleen and liver uptake after 15 min was followed by a gradual increase over 4 hrs. Also, a constant decrease in bladder activity was observed over 4 hrs. Significantly low percent specific uptake compared to liver, kidney, spleen and bladder uptake was observed in all the other organs which was found to decrease gradually over 4 hrs. Uptake in normal colon and stomach did not change significantly with time but it increased up to 2 hrs in colon tumor tissue, and then decreased to significantly low levels. Uptake in colon tumor increased gradually from 0.25 to 3 hrs but remained constant in normal colon from 0.25 to 4 hrs. Concomitant with the biodistribution pattern, the SPECT imaging (Figure 6a) confirmed the

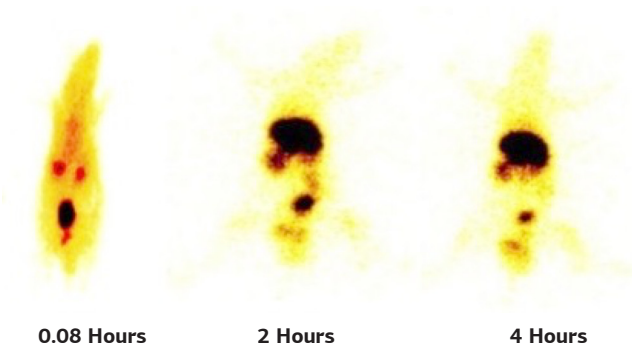

Figure 4. SPECT images (imaging of albumin tagged ^{99m}TC resveratrol). Static images of rats were obtained at 0.08 hrs (5 min), 2 and 4 hrs post i.v. administration.

accumulation of the activity in liver, spleen and colon tumor after 4 hrs (Figure 6b). High uptake by kidneys was observed initially after 15 min that then decreased at 4 hrs. Also, the lower left hand side panel of Figure 6b shows a magnified view of 4-hr view and confirms higher tumor specificity of albumin tagged ^{99m}-resveratrol.

Discussion

Albumin is emerging as a versatile protein carrier for drug targeting and for improving the pharmacokinetic profile of various drugs. The serum albumin is an efficient nano sized drug deliv-

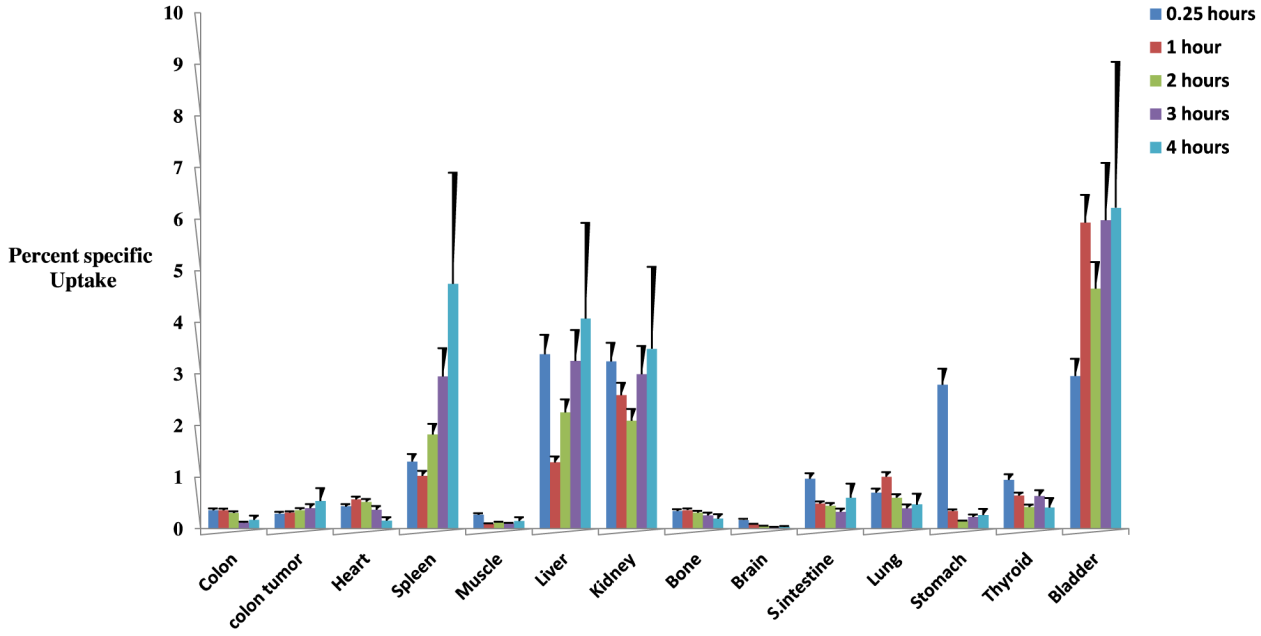

Figure 5. Biodistribution and imaging of albumin tagged ^{99m}TC resveratrol (SPECT). The radiotracer was quickly taken up by the liver, spleen, kidneys and soon appeared in urine (urinary bladder) after 15 min of i.v. injection.

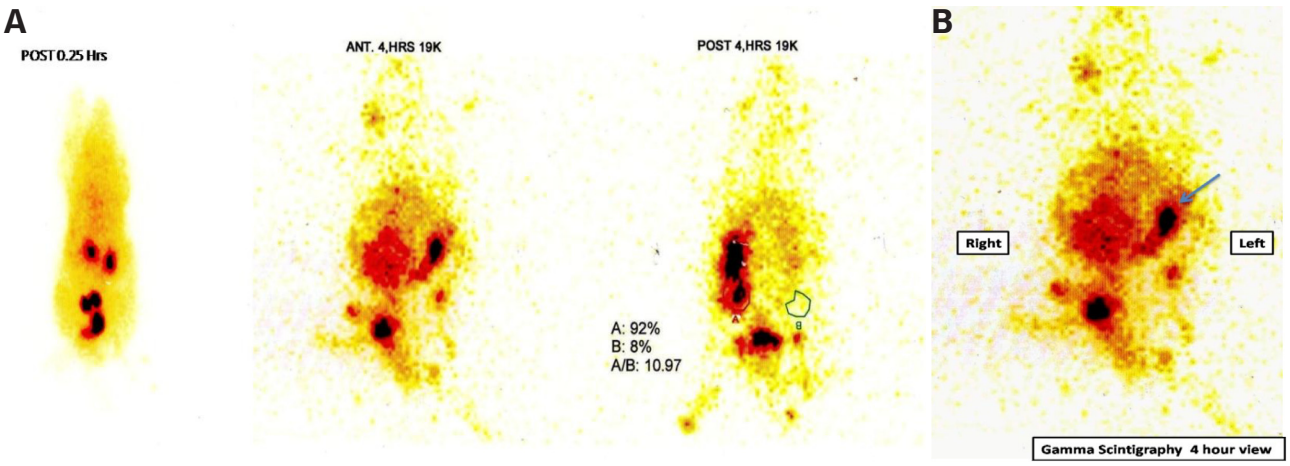

Figure 6. (A) Imaging of albumin tagged ^{99m}TC resveratrol. The SPECT imaging confirmed the accumulation of the activity in liver, spleen and colon tumor after 4 hrs. **(B)** Imaging of albumin tagged ^{99m}TC resveratrol after 4 hours (SPECT). This figure shows a magnified 4-hr view and confirms higher tumor specificity of albumin tagged ^{99m}-resveratrol.

ery system that offers preferential delivery at the tumor site. Serum albumin has been confirmed to be equipped with multiple molecular transporting mechanisms. The primarily reported transport mechanism is caveolin-mediated endocytosis, coupled with endosomal escape. The caveolin mediated encocytosis include gp60 (albodin) receptors that are extensively expressed in tumors as a result of high expression of cavelion-1 gene [16-19]. So, high concentrations of albumin receptors at the tumor site significantly elevated the uptake of the formed complex in the colon tumors of group II animals. Earlier studies also reported similar rise in uptake of paclitaxel after tagging with albumin [19,20]. The secreted protein acidic and rich in cysteine factor (SPARC) is a second mechanism responsible for increased target specific localization of albumin-tagged ^{99m}Tc-resveratrol in colon tumors. SPARC is basically a secreted protein acidic and rich in cysteine, and is highly expressed in variety of tumors [21,22]. So, this factor also created additional sink for albumin at the tumor site due to its high affinity for albumin. The above factors collectively contributed towards increased and specific localization of the albumin bound ^{99m}Tc-resveratrol in gastric tumors in comparison to gold nanoparticles. A recent study by Sarett et al. also utilized long-lived endogenous serum albumin as a carrier [23]. Some recent studies exploited cationic bovine serum albumin (CBSA)-based self-assembled nanoparticles for the delivery of chemotherapy drugs during metastatic lung cancer [24,25]. The present study showed for the first time that albumin tagged ^{99m}TC-resveratrol is more efficient over gold nanoparticles loaded ^{99m}TC-resveratrol in terms of both specificity as well as efficacy. In this way, this strategy could be extended to the clinical settings for the future development of advanced cancer therapeutics.

Conclusion

Albumin is a superior nanoparticle for delivery purposes over gold nanoparticles. However, future studies are essential for the extension of this technology for clinical applications.

Conflict of interests

The authors declare no conflict of interests.

References

1. Grégoire V, Thorwarth D, Lee JA. Molecular Imaging-Guided Radiotherapy for the Treatment of Head-and-Neck Squamous Cell Carcinoma: Does it Fulfill the Promises? Semin Radiat Oncol 2018;28:35-45.
2. Zhou K, Ding Y, Vuletic I et al. In vivo long term investigation of tumor bearing mKate2 by an in-hose fluorescence molecular imaging system. Biomed Eng Online 2018;17:187.
3. Salmanoglu E, Kim S, Thakur ML. Currently Available Radiopharmaceuticals for Imaging Infection and the Holy Grail. Semin Nucl Med 2018;48:86-99
4. Feng Y, Zhou J, Jiang Y. Resveratrol in lung cancer- a systematic review. J BUON 2016;21:950-3. Review.
5. Ferraresi A, Phadngam S, Morani F, Galetto A, Alabiso O, Chiorino G, Isidoro C. Resveratrol inhibits IL-6-induced ovarian cancer cell migration through epigenetic up-regulation of autophagy. Mol Carcinog 2017;56:1164-81.
6. Chaturvedi S, Mishra AK. Small Molecule Radiopharmaceuticals - A Review of Current Approaches. Front Med (Lausanne). 2016;3:5.
7. Fan Y, Yi J, Zhang Y, Yokoyama W. Fabrication of curcumin-loaded bovine serum albumin (BSA)-dextran nanoparticles and the cellular antioxidant activity. Food Chem 2018;239:12.
8. Djokic D, Jankovic D, Maksin T. Radiochemical purity and particles number determination of modified 99mTC-macroagreagated albumin. J Serb Chem 2002;67:573-9.
9. Ye BL, Zheng R, Ruan XJ, Zheng ZH, Cai HJ. Chitosan-coated doxorubicin nano-particles drug delivery system inhibits cell growth of liver cancer via p53/PRC1 pathway. Biochem Biophys Res Commun 2018;495: 414-20.
10. Mary Lazer L, Sadhasivam B, Palaniyandi K et al. Chitosan-based nano-formulation enhances the anticancer efficacy of hesperetin. Int J Biol Macromol 2018;107(Pt B):1988-99.
11. Daraee H, Eatemadi A, Abbasi E, Fekri Aval S, Kouhi M, Akbarzadeh A. Application of gold nanoparticles in biomedical and drug delivery. Artif Cells Nanomed Biotechnol 2016;44:410-22.
12. Johnston HJ, Hutchison G, Christensen FM, Peters S, Hankin S, Stone V. A review of the in vivo and in vitro toxicity of silver and gold particulates: particle attributes and biological mechanisms responsible for the observed toxicity. Crit Rev Toxicol 2010;40: 328-46.
13. Downs TR, Crosby ME, Hu T et al. Silica nanoparticles administered at the maximum tolerated dose induce

genotoxic effects through an inflammatory reaction while gold nanoparticles do not. Mutat Res 2012;745: 38-50.

14. Soler AP, Miller RD, Laughlin KV, Carp NZ, Klurfeld DM, Mullin JM. Increased tight junctional permeability is associated with the development of gastric cancer. Carcinogenesis 1999;20:1425-31.
15. Nune SK, Chanda N, Shukla R et al. Green Nanotechnology from Tea: Phytochemicals in Tea as Building Blocks for Production of Biocompatible Gold Nanoparticles. J Mater Chem 2009;19:2912-20.
16. Fung KYY, Fairn GD, Lee WL. Transcellular vesicular transport in epithelial and endothelial cells: Challenges and opportunities. Traffic 2018;19:5-18.
17. Chanthick C, Suttitheptumrong A, Rawarak N, Pattanakitsakul SN. Transcytosis Involvement in Transport System and Endothelial Permeability of Vascular Leakage during Dengue Virus Infection. Viruses 2018;10(2). pii: E69.
18. Mocan L, Matea C, Tabaran FA et al. Photothermal treatment of liver cancer with albumin-conjugated gold nanoparticles initiates Golgi Apparatus-ER dysfunction and caspase-3 apoptotic pathway activation by selective targeting of Gp60 receptor. Int J Nanomedicine 2015;10:5435-45.
19. Gradishar WJ, Tjulandin S, Davidson N et al. Phase III trial of nanoparticle albumin-bound paclitaxel compared with polyethylated castor oil-based paclitaxel in women with breast cancer. J Clin Oncol 2005;23:7794-803.
20. Desai N, Trieu V, Yao Z et al. Increased antitumor activity, intratumor paclitaxel concentrations, and endothelial cell transport of cremophor-free, albumin-bound paclitaxel, ABI-007, compared with cremophor-based paclitaxel. Clin Cancer Res 2006;12:1317-24.
21. Vaz J, Ansari D, Sasor A, Andersson R. SPARC: A Potential Prognostic and Therapeutic Target in Pancreatic Cancer. Pancreas 2015;44:1024-35.
22. Zhu A, Yuan P, Du F et al. SPARC overexpression in primary tumors correlates with disease recurrence and overall survival in patients with triple negative breast cancer. Oncotarget 2016;7:76628-34.
23. Sarett SM, Werfel TA, Lee L et al. Lipophilic siRNA targets albumin in situ and promotes bioavailability, tumor penetration, and carrier-free gene silencing. Proc Natl Acad Sci U S A 2017;114:E6490-E7.
24. Han J, Wang Q, Zhang Z, Gong T, Sun X. Cationic bovine serum albumin based self-assembled nanoparticles as siRNA delivery vector for treating lung metastatic cancer. Small 2014;10:524-35.
25. Chatterjee S, Lukas C. Heukamp, Maike Siobal et al. Tumor VEGF:VEGFR2 autocrine feed-forward loop triggers angiogenesis in lung cancer. J Clin Invest 2013;123:1732-40.